Carbon-vacancy concentration dependencies of electrical properties of NbC_x single crystals

1992 J. Phys.: Condens. Matter 4 8593

(http://iopscience.iop.org/0953-8984/4/44/020)

J. Phys.: Condens. Matter 4 (1992) 8593–8598. Printed in the UK

Carbon-vacancy concentration dependences of electrical properties of NbC_x single crystals

Yoshio Ishizawa, Shigeki Otani, Hiroshi Nozaki and Takaho Tanaka

National Institute for Research in Inorganic Materials, Namiki 1-1, Tsukuba, Ibaraki 305, Japan

Received 26 June 1992

Abstract. Electrical resistivities and the Hall effect of NbC_x single crystals (x = 0.71–0.975) have been studied with increasing carbon-vacancy concentration. Vacancy concentration dependences of the residual resistivities have been interpreted in terms of both x-dependent carrier densities and the electron–vacancy interaction where the Nordheim rule was applied. A difference in resistivity between 4.2 K and room temperature has also been explained in terms of additional x-dependent Debye temperatures and temperature-dependent anisotropy constants of the relaxation time. This model is also applied to TiC_x.

1. Introduction

Transition metal carbides with the NaCl-type structure can accommodate 25–45% vacancies on the carbon sublattice. Their characteristic properties such as high melting points, great hardness and high electrical and thermal conductivities depend strongly on the carbon-vacancy concentration. Electrical properties have been reported so far for TiC and other carbides mainly in a polycrystalline form and a few single crystal forms [1–7].

Systematic studies on electrical properties of IVa and Va group carbides should make clear the effect of carbon vacancies on the mechanism of transport phenomena. Such a systematic study using various compositions of TiC_x single crystals showed interesting resistivity behaviour [4]. The residual resistivity increases first with increasing vacancy concentration and then decreases a little for vacancy concentrations above about 20%. A more interesting phenomenon is the temperature coefficient of the resistivity, $d\rho/dT$, at room temperature firstly decreasing with increasing vacancy concentration and then the resistivity becoming almost temperature independent for vacancy concentrations of about 20%. Finally $d\rho/dT$ slightly increases again at higher vacancy concentrations. These behaviours of TiC_x single crystals were interpreted in terms of the vacancy-dependent carrier density and by applying Nordheim's rule to carrier–vacancy interaction, and by an increase in carrier density with increasing temperature. In this paper, NbC was selected to study the vacancy effect on resistivities and the Hall effect, and analysed using a common model which is considered to be general among the transition metal carbides with the NaCl-type structure.

0953-8984/92/448593+06$07.50

2. Experimental procedures

Single crystals of NbC_x were prepared by the zone-levelling floating zone technique [8–10]. Using this technique, we can grow single crystals with the desired and highly homogeneous chemical composition. The single-crystal rod is about 6 cm long and 9 mm in diameter. Carbon content was analysed using a carbon analyser (LECO, WR-12). The experimental error in composition (x = carbon to metal ratios) is within ±0.5%. The crystal structure of grown crystals was confirmed to be of NaCl type without any presence of long-range order of vacancies. The sample with $x = 0.71$ indicated the presence of some short-range ordering, but the effect of short-range ordering on electrical resistivities and the Hall effect is extremely small so we neglected this effect. Samples for measurements were cut from the single-crystal rod using a spark erosion machine. The rectangular samples, with dimensions of 1 mm × 1 mm × (7–8) mm, were etched before the measurements in a mixture of hydrofluoric and nitric acids at room temperature. Electrical currents were passed along the ⟨100⟩ direction. The electrical resistivity and the Hall effect measurements were performed from liquid helium temperature to room temperature using standard techniques.

3. Results and discussion

3.1. Vacancy concentration dependence of residual resistivities of NbC_x single crystals

Figure 1 shows temperature dependences of electrical resistivities of NbC_x with different carbon-vacancy concentrations in the temperature range from liquid helium to room temperature. As shown in figure 1, NbC is a superconductor with maximum T_c of 11 K which depends on the vacancy concentration. Here we focus on electrical resistivities. With increasing vacancy concentration, the residual resistivity increases and the temperature coefficient decreases.

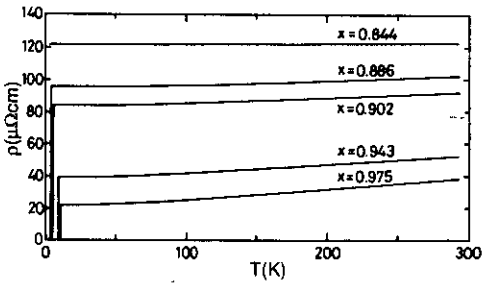

Figure 1. Electrical resistivities of NbC_x with different carbon-vacancy concentrations.

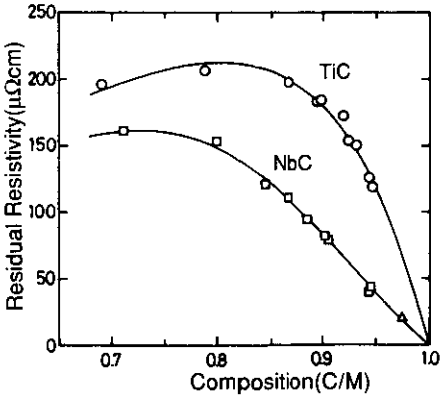

Figure 2. Vacancy concentration dependences of residual electrical resistivities of NbC_x and TiC_x. Solid curves are calculated ones which were least-squares fitted to data using the equations explained in the text.

In order to diminish the scattering of conduction electrons by phonons and to study effects due only to carbon vacancies, the resistivities of single crystals were measured at low temperatures, in the residual resistivity temperature range. Detailed results on the vacancy concentration dependence of residual resistivities of NbC_x are shown in figure 2 together with data for TiC_x. The open triangle shown in the data for NbC_x represents a polycrystalline sample with a maximum carbon content ($x = 0.975$) which was taken from a part of a solidified molten zone. As seen in figure 2, the initial resistivity increase due to the carbon vacancy in NbC_x is 8 $\mu\Omega$ cm/at.% V_c, where V_c is the carbon-vacancy concentration. The maximum resistivity of 160 $\mu\Omega$ cm was observed at $x \approx 0.7$. The residual resistivity with $x = 1.0$ was estimated to be nearly zero. This indicates that the scattering due to impurities or other imperfections is one or two orders smaller, and the main scattering is due to carbon vacancies as expected. The carrier density of $NbC(x = 1)$ at room temperature is estimated to be about one per formula unit from present measurements on the Hall effect which are discussed later. The band structure calculation [11] also supports this picture. Thus we adopt a single-carrier model to simplify the expression. Residual resistivity ρ_d is described by the following equation:

$$\rho_d = x(1-x)\delta/N. \tag{1}$$

Here, δ is a proportionality constant and N is the carrier density of conduction electrons. We applied the Nordheim rule as a scattering term due to the carbon vacancy [4]. That is, $1/\tau_d \propto x(1-x)$ where τ_d is relaxation time due to the carbon vacancy. The carrier density, N, depends on the vacancy concentration. In NbC,

$$N(x) = [n^{1/3} + \alpha x(x-\beta)^2]^3. \tag{2}$$

The n, α and β are adjustable parameters. This expression is easily obtained from the density of states (D) at the Fermi energy against vacancy concentration relation [11]. Here we assumed a simple expression for the x-dependence of D:

$$D(x) = \text{constant} + \alpha x(x-\beta)^2. \tag{3}$$

The solid line in figure 2 is a least-squares fit to the experimental data using the above equations. In order to determine the values of parameters which we used, we assume the carrier densities of $NbC(x = 1.0)$ at 4.2 K to be 1.0 per formula unit. Then, the δ value of NbC is determined as 690.17 from the determined parameters. Other parameters obtained are $n = 0.72$, $\alpha = 4.643$ and $\beta = 0.85$. The experimental values and the calculated line agree well, as expected. Thus the residual resistivities of NbC_x could be explained on the basis of both the scattering of conduction electrons by the carbon vacancies and the change in the carrier density due to the introduction of carbon vacancies.

3.2. Vacancy concentration dependence of the resistivity difference between 4.2 K and room temperature

Temperature dependences of electrical resistivities of carbides with the NaCl-type structure are very attractive to study because the temperature gradient decreases with increasing vacancy concentration, reaching an almost temperature-independent resistivity and then with further increase in the vacancy concentration, the temperature

gradient again appears. The Bloch–Gruneisen expression and the empirically determined equation were applied to explain the temperature dependences of some IVa and Va carbides with low vacancy concentration [5–7], but the case of almost temperature-independent resistivity with high vacancy concentration was not treated. In this case, some models have been proposed for TiC [3, 4]. For the case of NbC, the resistivity difference between 4.2 K and room temperature, $\Delta\rho(x) = \rho(\mathrm{RT}) - \rho_d$, has been investigated as a function of the vacancy concentration. The present model, in principle, should explain the temperature dependence over a wide range of vacancy concentrations.

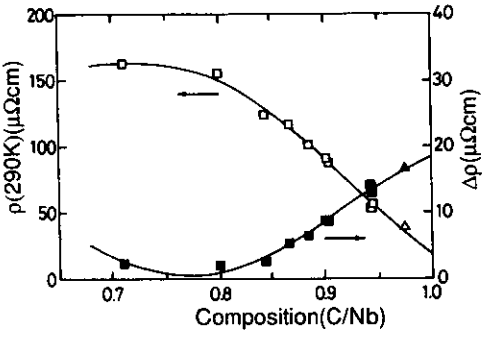

Figure 3. Vacancy concentration dependences of the room temperature resistivity and the resistivity difference between 4.2 K and room temperature of NbC_x. Solid curves in ρ(290 K) and $\Delta\rho$ are calculated ones which were least-squares fitted to the data using the equations explained in the text. The triangles represent polycrystalline samples with $x = 0.975$.

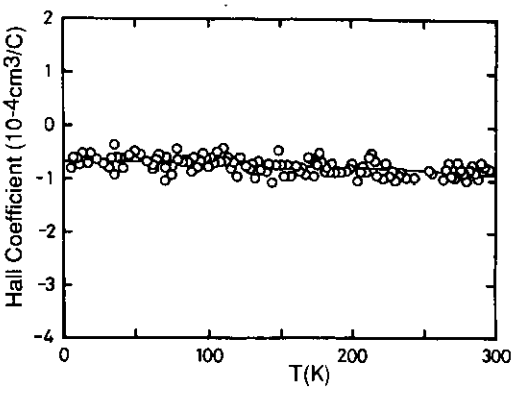

Figure 4. The temperature dependence of the Hall effect of $NbC(x = 0.946)$.

Experimental results on NbC_x are presented in figure 3. $\Delta\rho(x)$ decreases with increasing vacancy concentration, but increases a little at $x < 0.8$. Here we introduce a general model which can be applicable to carbides with the NaCl-type structure. In these carbides, residual resistivities are large at low temperature and electron–phonon interactions become important at room temperature. This means that the anisotropy constant of relaxation time changes with temperature, as for alloys [12, 13]. The following model is proposed using parameters of the anisotropy constants of the relaxation time. The equation is as follows:

$$\begin{aligned}\Delta\rho(x) &= (B/N)[(1/\tau_p + 1/\tau_d)/A_r - (1/\tau_d)/A_d] \\ &= (B/NA_r)[(1/\tau_p) - ((A_r - A_d)/A_d)(1/\tau_d)] \\ &= (a/N)[1/(x+b)^2 - cx(1-x)]. \end{aligned} \tag{4}$$

where $B = m/e^2$, and τ_p is relaxation time due to phonons. Parameters A_d and A_r are anisotropy constants of the relaxation time at 4.2 K and room temperature, respectively. Parameters a, b and c are adjustable constants to fit the data by the least-squares method.

The first term in (4) is the phonon scattering term which is derived from the experimental observation that Debye temperatures change with $(1 - x)$ [14]; that is, $1/\tau_p \propto 1/(x + b)^2$. The second term results from the temperature-dependent anisotropy constant: $c \propto (A_r - A_d)/A_d$. If $c = 0$ $(A_r = A_d)$, or $1/\tau_p$ is independent of the composition, then the experimental results cannot be explained. Assuming that A_r and A_d are x-independent for simplicity, we can fit the data using equation (4). The calculated curve in $\Delta\rho$ is shown as a solid line in figure 3. Parameters obtained are $a = 13.78$, $b = -0.1353$ and $c = 13.85$. The calculated curve of ρ(RT) is derived from the sum of $\Delta\rho$(cal) and ρ_d(cal).

3.3. The Hall effect of NbC_x

Figure 4 shows the temperature dependence of the Hall effect of NbC with $x = 0.946$. The Hall coefficients are negative and their absolute values are 0.62 and 0.88 in units of 10^{-4} cm^3 C^{-1} at 4.2 K and 290 K respectively. This indicates $A_r > A_d$, that is $c > 0$. This tendency holds over the entire composition range. Figure 5 shows the vacancy concentration dependences of the Hall coefficients at 4.2 K and 290 K. The circles and triangles in figure 5 represent the present data, but the triangles represent data estimated from the low- or high-temperature sides. The solid squares represent data taken at room temperature from Allison and Modine [5]. The solid curves were calculated using $N(x)$ with adjustable parameters to produce good fits.

3.4. Application to TiC_x

Previous data on the vacancy concentration dependence of the residual resistivity of TiC_x are shown in figure 2 [4]. We try to explain the experimental data qualitatively using the same model as used for NbC. As shown in figure 2, the initial resistivity increase due to the carbon vacancy is 24 $\mu\Omega$ cm/at.% V_c. This is three times higher than that of NbC_x. The maximum resistivity of 210 $\mu\Omega$ cm was observed at $x \approx 0.8$. The resistivity decreases with increasing carbon vacancy content ($x < 0.8$). The residual resistivity is explained by equation (1), and in TiC,

$$N(x) = [n^{1/3} + \alpha(1 - x)]^3. \tag{5}$$

The n and α are adjustable parameters. This expression is easily obtained from the density of states against the vacancy concentration relation [15]. The solid line in figure 2 is a least-squares fit to the experimental data. If we assume the carrier density $N(x = 1)$ to be 0.05 per formula unit, at low temperature, taking into consideration the measured Hall coefficient [7], then we have a δ value of 160.7. Other parameters are $n = 0.05$ and $\alpha = 0.629$. The smaller δ value of TiC_x is interpreted as being mainly due to the smaller effective mass of conduction electrons than for those in NbC_x. Furthermore, it is easily derived that the marked decrease in resistivity below $x = 0.8$ in TiC is due to a marked increase in carrier density compared with that of the stoichiometric composition. This effect is smaller in NbC because of a smaller change in carrier density with increasing vacancy concentration.

Vacancy concentration dependences of the room temperature resistivity and the resistivity difference between 4.2 K and room temperature in TiC_x are shown in figure 6 [4]. These data were adjusted to equation (4). The solid lines in figure 6 are calculated ones. This least-squares fitting gives the parameters $a = 0.7093$, $b = -0.3171$, $c = 24.30$. Agreement between experimental data and calculated curves is quite good. This indicates that the carbon vacancy effect on the transport properties of TiC is qualitatively the same as those for NbC.

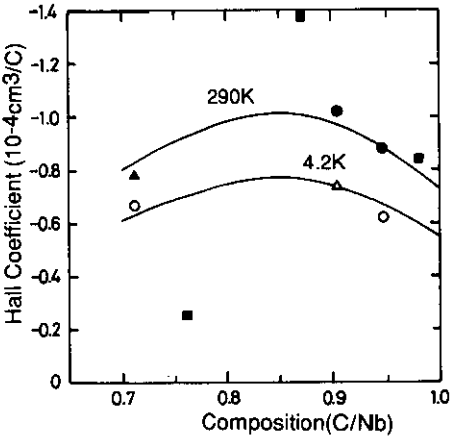

Figure 5. Vacancy concentration dependences of the Hall coefficients at 4.2 K and 290 K of NbC_x. The circles and triangles represent the present data and the solid squares represent the room temperature data from [5]. Solid curves were calculated using $N(x)$ using adjustable parameters to get good fits.

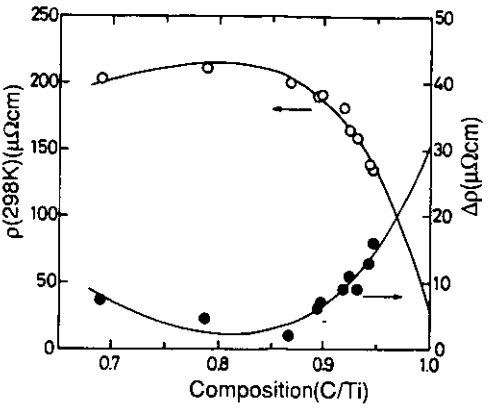

Figure 6. Vacancy concentration dependences of the room temperature resistivity and the resistivity difference between 4.2 K and room temperature of TiC_x. Solid curves for ρ(298 K) and $\Delta\rho$ are calculated ones which were least-squares fitted to the data using the equations explained in the text.

4. Conclusion

Vacancy concentration dependences of the electrical resistivity and the Hall coefficient of NbC_x single crystals have been interpreted from both x-dependent carrier densities and the electron–vacancy interaction where the Nordheim rule was applied. The difference in resistivity between 4.2 K and room temperature has also been explained by additional x-dependent Debye temperatures and temperature-dependent anisotropy constants of the relaxation time. This model was also applied to TiC_x, leading to the general model of transport phenomena of transition metal carbides with the NaCl-type structure.

References

[1] Williams W S 1964 *Phys. Rev.* A **135** 505
[2] Santro G and Dolloff R T 1968 *J. Appl. Phys.* **39** 2293
[3] Williams W S 1971 *Progress in Solid State Chemistry* vol 6 (Oxford: Pergamon) p 57
[4] Otani S, Tanaka T and Ishizawa Y 1986 *J. Mater. Sci.* **21** 1011
[5] Allison C Y, Modine F A and French R H 1987 *Phys. Rev.* B **35** 2573
[6] Allison C Y, Finch C B, Foegelle M D and Modine F A 1988 *Solid State Commun.* **68** 387
[7] Modine F A, Foegelle M D, Finch C B and Allison C Y 1989 *Phys. Rev.* B **40** 9558
[8] Otani S, Tanaka T and Ishizawa Y 1983 *J. Cryst. Growth* **61** 1
[9] Otani S, Tanaka T and Ishizawa Y 1983 *J. Cryst. Growth* **62** 211
[10] Otani S, Tanaka T and Ishizawa Y 1985 *J. Cryst. Growth* **71** 615
[11] Marksteiner P, Weinberger P, Neckel A, Zeller R and Dederichs P H 1986 *Phys. Rev.* B **33** 6709
[12] Kimura H and Honda K 1971 *J. Phys. Soc. Japan* **31** 129
[13] Cox W R, Hayes D J and Brotzen F R 1973 *Phys. Rev.* B **7** 3580
[14] Toth L E, Ishikawa M and Chang Y A 1968 *Acta Metall.* **16** 1183
[15] Marksteiner P, Weinberger P, Neckel A, Zeller R and Dederichs P H 1986 *Phys. Rev.* B **33** 812